Kr L X-ray and Au M X-ray emission for 1.5 MeV–3.9 MeV Kr^{13+} ions impacting on an Au target*

Mei Ce-Xiang(梅策香)[a)b)†], Zhang Xiao-An(张小安)[b)], Zhao Yong-Tao(赵永涛)[c)], Zhou Xian-Ming(周贤明)[c)], Ren Jie-Ru(任洁茹)[c)], Wang Xing(王 兴)[c)], Lei Yu(雷 瑜)[c)], Sun Yuan-Bo(孙渊博)[c)], Cheng Rui(程 锐)[c)], Wang Yu-Yu(王瑜玉)[c)], Liang Chang-Hui(梁昌慧)[b)], Li Yao-Zong(李耀宗)[b)], and Xiao Guo-Qing(肖国青)[c)]

[a)] *Department of Applied Physics, Xi'an Jiaotong University, Xi'an* 710049, *China*

[b)] *Ion Beam & Optical Physical Joint Laboratory of Xianyang Normal University and Institute of Modern Physics, Chinese Academy of Sciences, Xianyang* 712000, *China*

[c)] *Institute of Modern Physics, Chinese Academy of Sciences, Lanzhou* 730000, *China*

(Received 5 January 2013; revised manuscript received 16 April 2013)

Kr L X-ray and Au M X-ray emission for Kr^{13+} ions with energies of 1.5 MeV and 3.9 MeV impacting on an Au target are investigated at heavy ion research facility in Lanzhou (HIRFL). The L-shell X-ray yield per ion of Kr is measured as a function of incident energy. In addition, Kr L X-ray production cross section is extracted from the yield and compared with the result obtained from the classical binary-encounter approximation (BEA) model. Furthermore, the intensity ratio of the Au $M_{\beta 3}$ to $M_{\alpha 1}$ X-ray is investigated as a function of incident energy.

Keywords: X-ray yield per ion, X-ray production cross section, intensity ratio

PACS: 34.80.Dp, 32.30.Rj, 79.20.Rf **DOI:** 10.1088/1674-1056/22/10/103403

1. Introduction

The investigation of atomic inner-shell process has made great progress during the last decades,[1–4] especially for the inner-shell ionization of target atoms impacted by protons or light ions. During the collisions of highly charged heavy ions with atoms, the inner-shell electrons are ionized, and the corresponding vacancies may be filled by X-ray emission, Auger transition or Coster–Kroning (CK) transitions. X-ray emission plays an important role in studying the interaction of particles with solid surfaces, which provides a fundamental understanding for the relevant interaction mechanisms. X-ray is also an effective tool for diagnosing plasma and studying the interaction of heavy ion beam with dense mater, stellar evolution, and interstellar environment.[5] In the inertial confinement fusion experiment, high Z material is always made into a hohlraum target, and the projectiles are heated by target X-ray radiation. How to increase the transfer efficiency of X-ray radiation from interaction between an ion beam and a hohlraum target[6,7] is a hot topic. Gold is an important target material in inertial confinement fusion experiments.

The X-ray production cross section is closely related to ion–atom collisions, which involves the complex multiple-body problem. Therefore, the quantum-mechanical Schrödinger equation cannot give an accurate analytical solution. Fortunately, various theoretical models have been developed to estimate the X-ray production cross section. For example, the plane-wave Born approximation (PWBA),[8] binary encounter approximation (BEA),[9] semi-classical approximation (SCA),[10] and the perturbed stationary state by taking into account energy loss, Coulomb deflection, and relativistic effects (ECPSSR)[11,12] are available and can give a reasonable prediction to the certain collisions. Guo *et al.*[13] measured the L X-ray production cross section of Dy and Sm by electron impact at energy of tens of keV and found that the experimental data were higher than the BEA prediction at lower energies and the experimental results were gradually closer to the BEA prediction at higher energies. Zhou *et al.*[14,15] and Wang *et al.*[16] have compared the X-ray emission of the target atom induced by protons with those by highly charged heavy ions, investigated the multiple ionization of the outer-shell electrons, and found that the BEA model with considering the multiple-ionization fluorescence yield presents the result in good agreement with the experimental cross section. Although much attention has been paid to the target atom X-ray production cross section, only a few works have studied the X-ray production cross section of the projectile. Not only are the experimental data needed, but also the theoretical model needs to be further developed. Here, we present the coinstantaneous investigation of the X-ray emission for the projectile and the target.

In this paper, the investigations of the X-ray emission for the projectile Kr and the target Au are performed for $^{36}Kr^{13+}$

*Project supported by the National Natural Science Foundation of China (Grant Nos. 11075135, 11075192, and 11075125) , the Scientific Research Foundation of the Education Department of Shaanxi Province, China (Grant No. 2010JK895), and the Special Foundation of Xianyang Normal University, China (Grant No. 11XSYK308).

†Corresponding author. E-mail: canoemei@163.com

© 2013 Chinese Physical Society and IOP Publishing Ltd

ions beams impacting on a gold target. Initial kinetic energies of the projectile are 1.5 MeV and 3.9 MeV, respectively. Yield per ion and the production cross section of a Kr L X-ray are discussed. Additionally, the target atom M X-ray is investigated.

2. Experimental setup

The experiment is performed on a 320-kV high voltage experimental platform using the electron cyclotron resonance ion source at the Institute of Modern Physics, Chinese Academy of Sciences in Lanzhou. The experimental setup is shown in Fig. 1. The ion beam is introduced into the ultrahigh vacuum target chamber (10^{-8} mbar, 1 bar = 10^5 Pa) by deflecting, focusing, and collimating it, becoming a spot size of about 3 mm×3 mm, and it impacts perpendicularly onto the target surface. The emitted X-rays are observed by using a silicon drift detector (XR-100SDD) with a beryllium vacuum window in the front. The distance of the detector to the target is 32.5 cm. The detector has an energy resolution of about 136 eV at an energy of 5.899 keV and an effective energy range of 0.7 keV–100 keV. A standard ^{55}Fe source calibrates the X-ray detector before and after the measurement. The geometrical solid angle is about (0.0066 ± 0.00013) sr. The Au target has a purity of 99.99% with a surface area of 15 mm×20 mm and thickness of 0.30 mm.

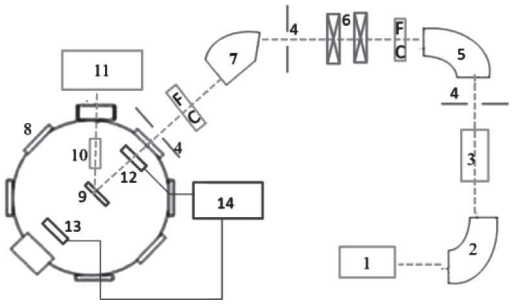


Fig. 1. Schematic drawing of the experimental setup.[15] 1: ECR ion source, 2: analyzing magnet, 3: high volt accelerate platform, 4: barrier, 5: 90° deflection magnet, 6: magnetic quadrupled lens, 7: 60° deflection magnet, 8: ultrahigh vacuum target chamber, 9: target, 10: silicon drift detector, 11: X-ray recording system, 12: penetrable faraday cup, 13: common faraday cup, 14: projectile number recording system.

3. Results and discussion

3.1. Characteristic of X-rays

Figure 2 shows the X-ray spectra induced by krypton ions with an energy of 3.9 MeV impacting on a gold target. The original spectrum is well fitted by using Gauss fitting. The lines at 1.656 keV and 1.862 keV have been identified as the characteristic L_α ($3d_{3/2,5/2}$–$2p_{3/2}$) and $L_{\beta 3,4}$ ($3p_{3/2}$, $3p_{1/2}$–$2s_{1/2}$) X-ray of Kr, respectively. The line at 2.185 keV has unambiguously been identified as Au M_α ($4f_{7/2}$–$3d_{5/2}$) X-ray. The Au $M_{\beta 3}$ ($4d_{5/2}$–$3p_{3/2}$) X-ray line is at 2.495 keV.

Table 1 lists the experimental energy values of X-rays when Kr^{13+} at 3.9 MeV impacts on a gold target. According to the X-Ray Data Booklet,[17] we list the theoretical energy values of those X-ray spectra. By comparing with the theoretical value, we observed that the experimental energy value of Kr L_α X-ray line shifts toward the higher energy by 70 eV. A lot of work have been done to study the multiple ionization by X-ray energy shift.[18,19] In the present work, the results are in accordance with our previous experimental results, in which the same target and different incident energy values were used.[20] In addition, we list the electron configuration transitions of different X-rays.

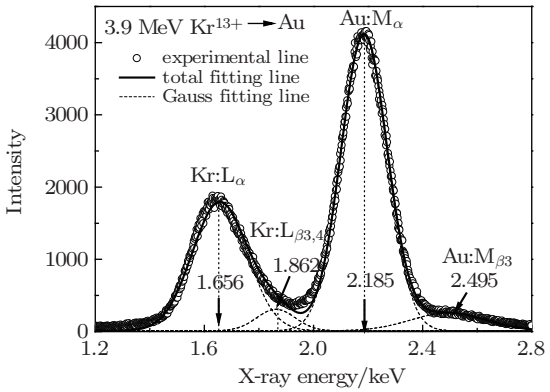


Fig. 2. X-ray spectra for Kr^{13+} ions with kinetic energy 3.9 MeV impacting on an Au target.

Table 1. Comparison between the experimental energy and the reference value of X rays.

X-ray spectra	Experimental energy/keV	Reference value[16]/keV	Electron configuration transition
Kr L_α	1.656	1.586	$3d_{3/2,5/2}$–$2p_{3/2}$
Kr $L_{\beta 1}$	1.656	1.636	$3d_{3/2}$–$2p_{1/2}$
Kr $L_{\beta 3,4}$	1.862	1.706	$3p_{3/2}$, $3p_{1/2}$–$2s_{1/2}$
Au $M_{\alpha 3}$	1.656	1.660	$4p_{1/2}$–$3d_{3/2}$
Au $M_{\alpha 1}$	2.185	2.123	$4f_{7/2}$–$3d_{5/2}$
Au $M_{\beta 3}$	2.495	2.408	$4d_{5/2}$–$3p_{3/2}$

According to the X-Ray Data Booklet,[17] the energy separation of Kr $L_{\beta 1}$ X-ray and Kr L_α X-ray is about 50 eV, which is beyond our detector resolution range. The intensity of Kr L_α X-ray is larger than that of Kr $L_{\beta 1}$, therefore we recognize the line at 1.656 keV as a Kr L_α X-ray line. In the present work, the Kr M-shell characteristic X-ray is not in the effective energy range of our detector. Therefore Kr M X rays are not observed in our experiments. In addition, Fig. 3 shows the characteristic X-ray spectra induced by Kr^{13+} ions with an energy of 3.9 MeV impacting on an Au target. One can find that the Kr K-shell X-ray and Au L-shell X rays are not observed. That is because the interaction energy between the target and the projectile is too small to excite Kr K-shell and Au L-shell electrons.

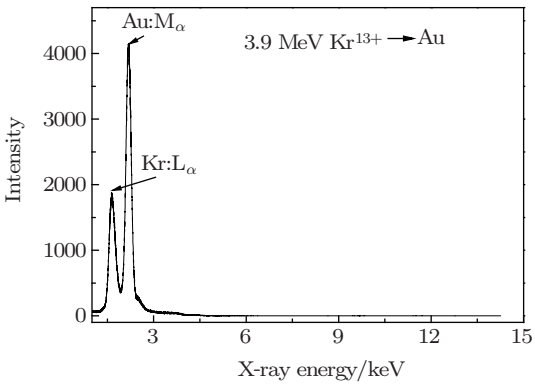


Fig. 3. X-ray spectra for Kr^{13+} ions impacting on an Au target.

3.2. Kr L X-ray yield per ion and production cross section

In this work, X-ray yield per ion is given by

$$Y(E) = \frac{N_x}{N_p \varepsilon(\Omega/4\pi)}, \tag{1}$$

where N_x is the observed X-ray count which is extracted from the Gauss fitting of the spectrum by nonlinear curve fitting procedures; N_p is the total number of incident ions, which could be calculated by $N_p = Q/q$, with Q being the integral intensity of the projectile charge and q being the initial charge state of the projectile; ε is detection efficiency at the corresponding X-ray energy, which is 51% for Kr L$_\alpha$; Ω is the solid angle of the detector. The main uncertainty of the yield originating from the statistics of the X-ray count is about 5%, and that of the measurement of the incident ion number is about 10%. The total uncertainty of the yield is about 11% after the error propagation. As shown in Table 2, with the increase of the incident energy, the production probability of the L-shell vacancies becomes bigger, therefore, Kr L X-ray yield increases with incident energy increasing.

Table 2. Kr L X-ray yields per ion versus incident energy.

Incident energy/MeV	Kr L X-ray yields per ion		
	Kr L$_\alpha$, L$_{\beta1}$	Kr L$_{\beta3,4}$	Total
1.5	8.59×10^{-5}	1.09×10^{-5}	9.68×10^{-5}
3.9	2.00×10^{-4}	2.34×10^{-5}	2.23×10^{-4}

The X-ray production cross section is derived from the X-ray yield using the standard formula

$$\sigma_x(E) = \frac{1}{N}\left[\frac{dY(E)}{dE}\cdot\frac{dE}{dR} + \frac{\cos\theta}{\cos\varphi}\mu Y(E)\right], \tag{2}$$

where N is the target atom density (atoms/g), μ is the mass absorption coefficient of the target for its own characteristic X-rays given by Grande *et al.*,[21] θ is the incident angle with respect to the normal direction of the target surface, ϕ is the observation angle with respect to the target normal, $Y(E)$ is the single ion yield at projectile energy E, dY/dE is extracted from fitting polynomials to E and $Y(E)$, dE/dR is the stopping power which can be obtained by SRIM [http://www.srim.org/]. The total uncertainty of the X-ray production cross section is below 20% after the error propagation.

The BEA model, which describes the inner-shell ionization as the classical collisions between the incident ions and the ionized electrons, calculate the ionization cross section for a definite energy transfer from the moving partials to the orbital electron of the atoms. The X-ray of the subshell can be calculated by the BEA model. The classical BEA prediction can be given in a close form as[9]

$$\sigma^{BEA} = \left(\frac{NZ^2\sigma_0}{U^2}\right)G(V), \tag{3}$$

where N is the electron number for the i-shell, Z is the projectile nuclear charge, σ_0 is equal to πe^4, U is the electron binding energy, $G(V)$ is a universal function of the scaled velocity V ($V = v_p/v_i$, where v_p is the velocity of the projectile, v_i the average velocity of the i-shell electron), $G(V)$ is approximately given by $4V^4/15$ when V is less than 0.206. During our calculation, we assume that the projectile is stationary and the target moves.

The relationship of the X-ray production cross section between L$_i$-subshell ($i = 1,2,\ldots$) and L$_\alpha$ (or L$_\beta$) can be calculated as follows:[22]

$$\sigma_{L_\alpha} = [\sigma_{L_1}(f_{12}+f_{23})+\sigma_{L_2}f_{23}+\sigma_{L_3}]\omega_3 S_{\alpha_3}, \tag{4}$$

$$\sigma_{L_\beta} = \sigma_{L_1}[\omega_1 S_{\beta_1}+f_{12}\omega_2 S_{\beta_2}+(f_{12}f_{23}+f_{13})\omega_3 S_{\beta_3}] + \sigma_{L_2}(\omega_2 S_{\beta_2}+f_{23}\omega_3 S_{\beta_3})+\sigma_{L_3}\omega_3 S_{\beta_3}, \tag{5}$$

where ω_i is the the fluorescence yield, f_{ij} is the Coster–Kronig yield, $S_{pi} = \Gamma_p/\Gamma_I$ is the fraction of the radiative transition to the i-th subshell associated with the L$_p$ peak. The parameter value is cited from Campbell.[23,24] The results of the Kr L X-ray production cross section measurements are given in Table 3, and compared with the predicted results with the BEA model.

Table 3. Comparison of Kr L X-ray production cross section between the experiment and the BEA model. The unit 1 b = 10^{-28} m^2.

Kr L X-ray line	Incident energy/MeV	$\sigma_x(E)$/b	$\sigma_x^{BEA}(E)$/b	$\sigma_x(E)/\sigma_x^{BEA}(E)$
Kr L$_\alpha$, L$_{\beta1}$	1.5	81.5	105.0	0.78
	3.9	285	713	0.40
Kr L$_{\beta3,4}$	1.5	9.82	0.72	13.64
	3.9	20.7	5.15	4.02

The Kr L$_\alpha$, L$_{\beta1}$ X-ray production cross section predicted by the BEA model is found to overestimate the measured data. The fluorescence yields obtained from Eqs. (4) and (5) do not take into account the multiple ionization effect of the projectiles which will increase the theoretical predictions for X-ray production. For the Kr L$_{\beta3,4}$ line, the experimental value is obviously larger than the BEA theoretical calculation value. The ratio of $\sigma_x(E)/\sigma_x^{BEA}(E)$ diminishes with the increase of incident energy. In experimental measurement, the areas of the Au M$_{\alpha3}$ ($4p_{1/2}$–$3d_{3/2}$) line and the Kr L$_{\beta3,4}$ line overlap,

and we remark it as the Kr $L_{\beta 3,4}$ line. As the relative intensity of Au $M_{\alpha 3}$ line is smaller than that of the Kr $L_{\beta 3,4}$ line and the energy separation of two lines is too small to be recognized by our detector, we neglect the Au $M_{\alpha 3}$. During the theoretical calculation of the X-ray production cross section for the Kr $L_{\beta 3,4}$ line, we do not consider the influence of the Au $M_{\alpha 3}$ X rays. Therefore, the experimental value is larger than the theoretical calculation. The ratio of $\sigma_x(E)/\sigma_x^{BEA}(E)$ decreases with incident energy increasing. It can be explained that a Kr $L_{\beta 3,4}$ X-ray is easily excited by higher energy, and the ratio of $I(\text{Au } M_{\alpha 3})/I(\text{Kr } L_{\beta 3,4})$ decreases with incident energy increasing. The larger the proportion of Kr $L_{\beta 3,4}$, the more contiguous the values between $\sigma_x(E)$ and $\sigma_x^{BEA}(E)$ are.

3.3. Au M X-ray emission

From Ref. [25], the potential energy threshold of Ar^{11+} for exciting Au atomic M_α X rays is 2.004 keV. In the present work, when an Au target is induced by Kr^{13+} ions, the Kr^{13+} which carries 2.037-keV potential energy will be deposited on the surface of the Au target and the $3d_{5/2}$ electrons in the M-subshell will be excited. In addition, the electrons in the M-subshell of the gold target are also excited by kinetic energy besides the potential energy of the projectiles. Figure 4 shows the X-ray spectra induced by krypton ions with 1.5 MeV and 3.9 MeV impacting on a gold target. From Fig. 4, Au $M_{\alpha 1}(4f_{7/2}–3d_{5/2})$ and Au $M_{\beta 3}(4d_{5/2}–3p_{3/2})$ are observed, indicating that the $3d_{5/2}$ and $3d_{3/2}$ electrons in M-shell are excited and the electrons in the N-shell fill up the M-shell holes.

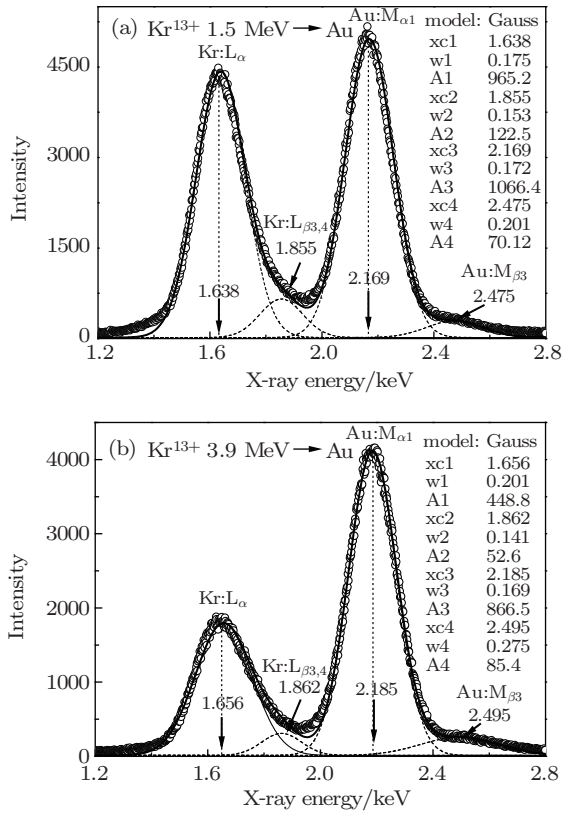


Fig. 4. The X-ray spectrum emission from the Kr^{13+} ions impacting on an Au target, (experimental line ○; total fitting line —; Gauss fitting line ⋯). The kinetic energy values of Kr^{13+} are (a) 1.5 MeV; (b) 3.9 MeV.

The results of the intensity ratio between Au $M_{\beta 3}$ and $M_{\alpha 1}$ lines are investigated and the results are listed in Table 4. It is found that the ratio of $I(M_{\beta 3})/I(M_{\alpha 1})$ has a little growth tendency with incident energy increasing, indicating that the bigger the incident energy, the more chance of Au $M_{\beta 3}(4d_{5/2}–3p_{3/2})$ emission. With the increase of incident energy, multiple ionization effects become visible. Because of multiple ionization effects in the N sub-shell, some CK transitions cannot take place.[26] Therefore the probability of radiative transition increases with the decrease of the CK transition probability. With the incident energy increasing, the probability of a vacancy occurring in the $3p_{3/2}$ sub-shell becomes bigger.

Table 4. Comparison of intensity between Au $M_{\alpha 1}$ and $M_{\beta 3}$ lines.

Incident ions (energy)	$I(M_{\alpha 1})$	$I(M_{\beta 3})$	$I(M_{\beta 3})/I(M_{\alpha 1})$
Kr^{13+} (1.5 MeV)	4984.06	323.62	0.065
Kr^{13+} (3.9 MeV)	4117.05	278.05	0.068

4. Conclusions

The Kr L X-ray and the Au M X-ray emission from the interaction of $^{36}Kr^{13+}$ ions with energies of 1.5 MeV and 3.9 MeV with an Au target are discussed in detail. Kr L X-ray yield per ion is calculated and the yield increases with incident energy increasing. The Kr L X-ray production cross section is also measured and compared with the result calculated by using the BEA theoretical model. Through comparison, it is found that the Kr L X-ray production cross section increases with incident energy increasing. It means that the larger the incident energy, the more easily the L-shell electrons of projectiles are ionized. In addition, the intensity ratio between Au $M_{\beta 3}$ and the $M_{\alpha 1}$ line increases only slightly with the increase of incident energy, which is attributed to an enhancement in M_3 subshell fluorescence yield, owing to multiple vacancies in N subshells.

References

[1] Czarnota M, Banaś D, Braziewicz J, Semaniak J, Pajek M, Jaskola M, Korman A, Trautmann D, Kretschmer W, Lapicki G and Mukoyama T 2009 *Phys. Rev. A* **79** 032710
[2] Zhang X A, Zhao Y T, Hoffmann D H H, Yang Z H, Chen X M, Xu Z F, Li F L and Xiao G Q 2011 *Laser Part. Beams* **29** 265
[3] Zhao Y T, Xiao G Q, Zhang X A, Yang Z H, Zhan W L, Chen X M and Li F L 2006 *Nucl. Instrum. Method B* **245** 72
[4] Burgdorfer J, Lerner P and Meyer F 1991 *Phys. Rev. A* **44** 5674
[5] Gregori G, Glenzer S H and Fournier K B 2008 *Phys. Rev. Lett.* **101** 045003
[6] Hoffmann D H H, Blazevic A, Korostiy S, Ni P, Pikuz S A, Rosmej O, Roth M, Tahir N A, Udrea S, Varentsov D, Weyrich K, Sharkov B Y and Maron Y 2007 *Nucl. Instrum. Method Phys. Res. Sec. A* **577** 8
[7] Yang Z R, Yuan P, Li Z W and Yang Z H 2012 *High Power Laser and Particle Beams* **24** 1896
[8] Mukoyama T 1986 *Bull. Inst. Chem. Res.* **64** 12
[9] Gryzinski M 1965 *Phys. Rev. A* **138** 336
[10] Hansteen J M and Mosebekk O P 1973 *Nucl. Phys. A* **201** 541

[11] Brandt W and Lapicki G 1981 *Phys. Rev. A* **23** 1717
[12] Lapicki G, Laubert R and Brandt W 1980 *Phys. Rev. A* **22** 1889
[13] Guo C J, Wu Z W, Yang D L, He Y Q, Peng X F, An Z and Luo Z M 2005 *Chin. Phys. Lett.* **22** 2244
[14] Zhou X M, Zhao Y T, Cheng R, Wang X, Lei Y, Sun Y B, Wang Y Y, Xu G, Ren J R, Zhang X A, Liang C H, Li Y Z, Mei C X and Xiao G Q 2013 *Acta Phys. Sin.* **62** 083201 (in Chinese)
[15] Zhou X M, Zhao Y T, Cheng R, Wang Y Y, Lei Y, Wang X and Sun Y B 2013 *Nucl. Instrum. Method B* **299** 61
[16] Wang X, Zhao Y T, Cheng R, Zhou X M, Xu G, Sun Y B, Lei Y, Wang Y Y, Ren J R, Yu Y, Li Y F, Zhang X A, Li Y Z, Liang C H and Xiao G Q 2012 *Acta Phys. Sin.* **61** 193201 (in Chinese)
[17] Thompson A C, Attwood D T, Gullikson E M, Howells M R, Kortright J B, Robinson A L and Underwood J H 2001 *Report on Second Edition Lawrence Berkeley National Laboratory,* University of California, USA
[18] Mitra D, Sarkar M, Bhattacharya D, Santra S, Mandal A C and Lapicki G 2010 *Nucl. Instrum. Method B* **268** 450
[19] Singh Y P, Misra D, Kadhane U and Tribedi L C 2006 *Phys. Rev. A* **73** 032712
[20] Mei C X, Zhao Y T, Zhang X A, Ren J R, Zhou X M, Wang X, Lei Y, Liang C H, Li Y Z and Xiao G Q 2012 *Laser Part. Beams* **30** 665
[21] Grande W H N K D, Mallett J H and Hubbell J H 1970, "1969 Compilation of X-ray Cross Sections", *Lawrence Livermore National Laboratory Report UCRL*-50174, USA
[22] Lapicki G, Murty G A V R, Raju G J N, Reddy B S, Reddy S B and Vijayan V 2004 *Phys. Rev. A* **70** 062718
[23] Campbell J L and Wang J X 1989 *At. Data Nucl. Data Tables* **43** 281
[24] Campbell J L 2003 *At. Data Nucl. Data Tables* **85** 291
[25] Zhang X A, Li Y Z, Zhao Y T, Liang C H, Cheng R, Zhou X M, Wang X, Lei Y, Sun Y B, Xu G, Li J Y and Xiao G Q 2012 *Acta Phys. Sin.* **61** 113401 (in Chinese)
[26] Wang X, Zhao Y T, Cheng R, Zhou X M, Xu G, Sun Y B, Lei Y, Wang Y Y, Ren J R, Yu Y, Li Y F, Zhang X A, Li Y Z, Liang C H and Xiao G Q 2012 *Phys. Lett. A* **376** 1197